

# 设计指南: TIDA-010050 适用于 AMR 的超低功耗水流测量参考设计



## 说明

此参考设计经过全面测试，展示了一个通过机械流量计对水流进行电子测量的低功耗解决方案，并提供了用于水流测量和无线通信的单芯片平台。该设计非常适用于水表自动抄表 (AMR) 模块，该模块可在现有机械流量计上添加无线通信功能。射频子系统支持无线 M-Bus 等标准协议或低于 1GHz ISM 频带的专有协议。此参考设计可提供远距离精确读取机械旋转量的能力，并提供更高的可靠性。超低的功耗可降低对电池的要求并延长产品寿命。

## 资源

<a href="#">TIDA-010050</a>	设计文件夹
<a href="#">CC1312R</a>	产品文件夹
<a href="#">CSD23285F5</a>	产品文件夹
<a href="#">SN74AUP2G00</a>	产品文件夹
<a href="#">LAUNCHXL-CC1312R1</a>	产品文件夹
<a href="#">Sensor Controller Studio</a>	产品文件夹

## 特性

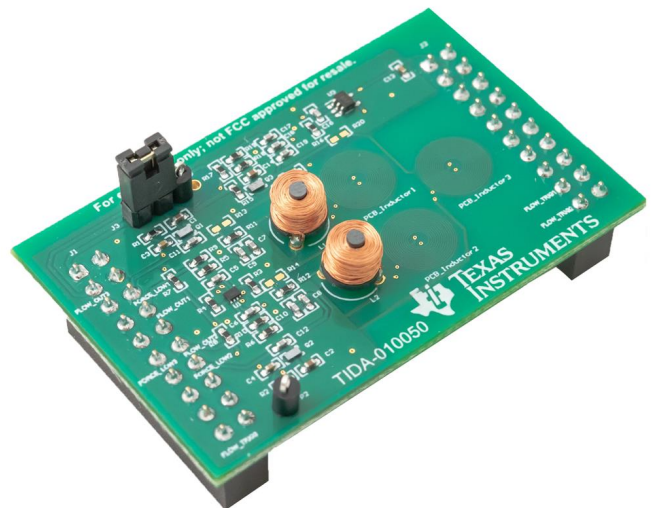
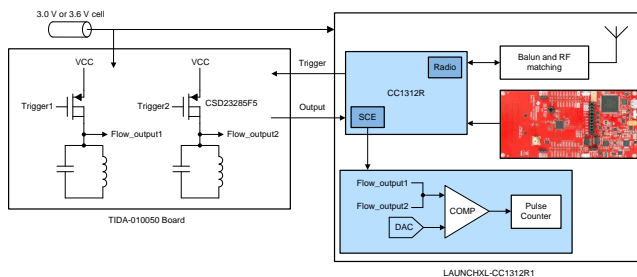
- 具有流量计计量和射频通信子系统的单芯片集成解决方案
- 满足 ISO4064-1:2014-11 (1 类) 测量精度要求
- 采样频率为 16Hz 且电源电压为 3.3V 时，消耗 1.83 $\mu$ A 的电流
- 可在距离旋转光盘高达 5.8mm 处进行精确测量
- 经完整测试且具有固件、设计文件和测试报告的参考设计

## 应用

- 电子 AMR 附加模块
  - 水表
  - 热量计
  - 燃气表



咨询我们的 E2E™ 专家



该 TI 参考设计末尾的重要声明表述了授权使用、知识产权问题和其他重要的免责声明和信息。

## 1 System Description

There is an increasing demand for the development of smart water meters from all over the world in replace of traditional mechanical meters. Compared with a full replacement of an electronic meter, using an electronic add-on module to integrate with the mechanical meters can be a less expensive solution. With the cost consideration and competitive performance, it can be placed in an increasingly strong position in the market.

The TIDA-010050 uses TI's CC1312R SimpleLink™ ultra-low-power wireless MCU to implement a LC-sensing subsystem to detect disc rotation with minimal cost while achieving extremely low power consumption without compromising on performance. This single-ship solution introduces a novel approach for flow measurement applications by integrating a true wireless AMR capability with low-cost LC sensors to deliver a highly affordable and physically compact solution. This reference design can be implemented with any CC13x2 and CC26x2 SimpleLink™ low-power RF wireless MCU, which integrates the same sensor controller engine.

The TIDA-010050 is a further development to the [Low-power water flow measurement with inductive sensing reference design](#), which is based on the CC13x0 device. Because there are lots of improvements tuned toward ultra-low power in the CC13x2, including a 2-MHz clock, fast wake-up, and ultra-low power counter, the power consumption of the TIDA-010050 is significantly lower. Several modifications in hardware and software have been validated to offer a better system performance of distance and accuracy detection, including inductor cross-coupling effect suppression and calibration mechanism during initialization.

### 1.1 Key System Specifications

表 1. Key System Specifications

PARAMETER	SPECIFICATIONS	DETAILS
Input voltage	2~3.8 V (Lithium-ion primary cell: Li-SOCL2 or LiMnO2)	<a href="#">4.2 节</a>
Sensor method	Inductive (or LC sensing)	<a href="#">2.4 节</a>
Average power consumption	1.83 $\mu$ A and 4.42 $\mu$ A with 16-Hz and 64-HZ sampling rate at 3.3 V, respectively (without interrupts to the system CPU application)	<a href="#">节 4.2.1</a>
Motion sensing range (distance between disc and inductor)	Maximum 5.8 mm with Gemphil inductor <a href="#">GT1302-0</a>	<a href="#">节 4.2.2</a>

## 2 System Overview

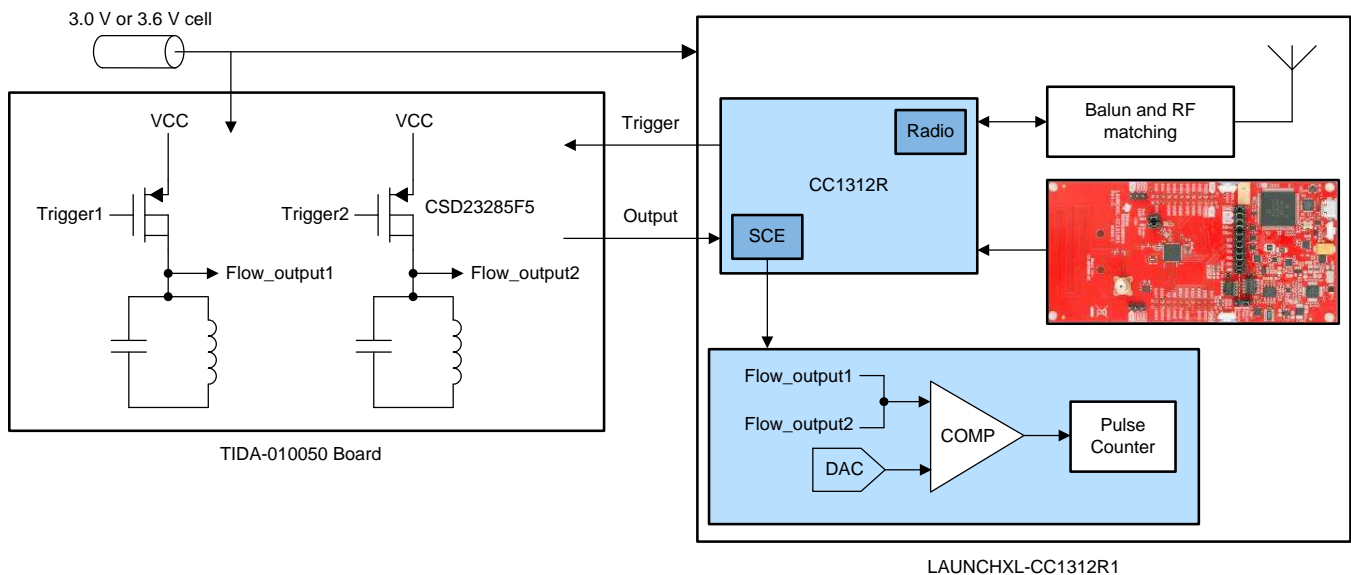
### 2.1 Block Diagram

As shown in 图 1, the TIDA-010050 is developed based on TI's SimpleLink™ MCU platform LAUNCHXL-CC1312R1, providing a simple platform for the evaluation of ultra-low power flow measurement applications.

The TIDA-010050 board is constructed with two LC sensors, as the detection interface to a half-metal, half non-metal disc in mechanical flow meters. A motor will be used to drive a rotor disc to simulate water flow. Two kinds of inductors, including the Gemphil inductor and PCB inductor, are provided in the design for evaluation.

Though primarily targeted at mechanical water meters, the TIDA-010050 can be used to update the traditional mechanical heat and cooling meters or gas meters as well.

图 1. TIDA-010050 Block Diagram



### 2.2 Highlighted Products

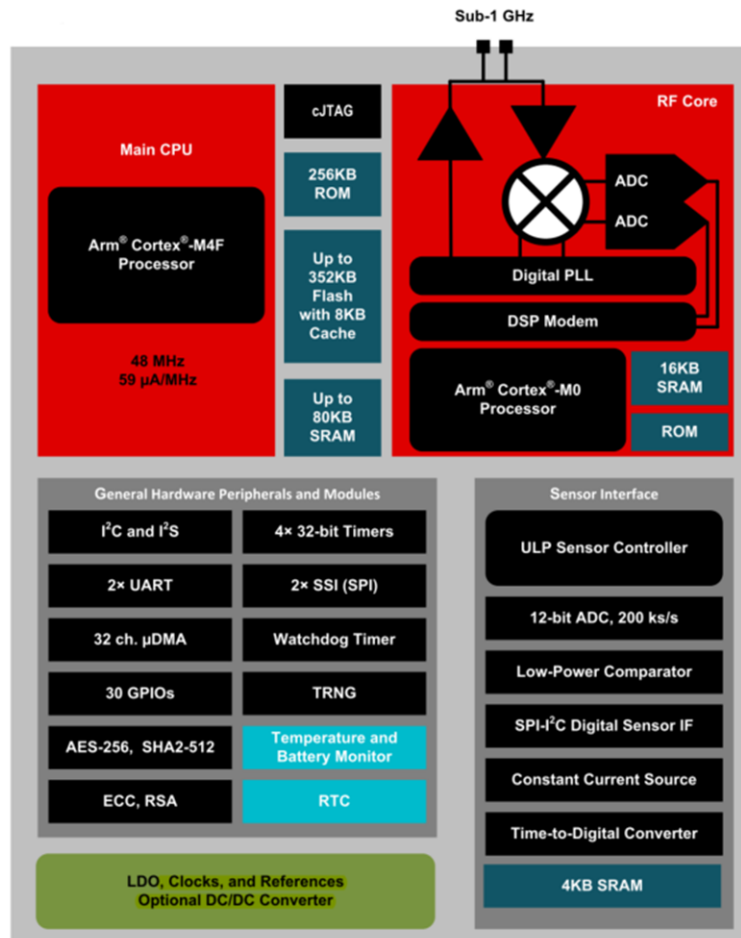
The TIDA-010050 contains two key devices: the CC1312R MCU and the FemtoFET CSD23285F5.

#### 2.2.1 CC1312R

The CC1312R device is a Sub-1 GHz wireless MCU targeting wireless M-Bus, IEEE 802.15.4g, IPv6-enabled smart objects (6LoWPAN), ZigBee®, KNX RF, Wi-SUN®, and proprietary systems.

The CC1312R device is a member of the CC13x2 and CC26x2 SimpleLink™ low-power RF wireless MCU products. This reference design can be applied with all CC13x2 and CC26x2 devices. As shown in 图 2, the CC1312R device combines a flexible, very low-power RF transceiver with a powerful 48-MHz Arm® Cortex®-M4F CPU in a platform supporting multiple physical layers and RF standards. A dedicated Radio Controller (Arm® Cortex®-M0) handles low-level RF protocol commands that are stored in ROM or RAM, thus ensuring ultra-low power and great flexibility. The low power consumption of the CC1312R device does not come at the expense of RF performance; the C1312R device has excellent sensitivity and robust performance.

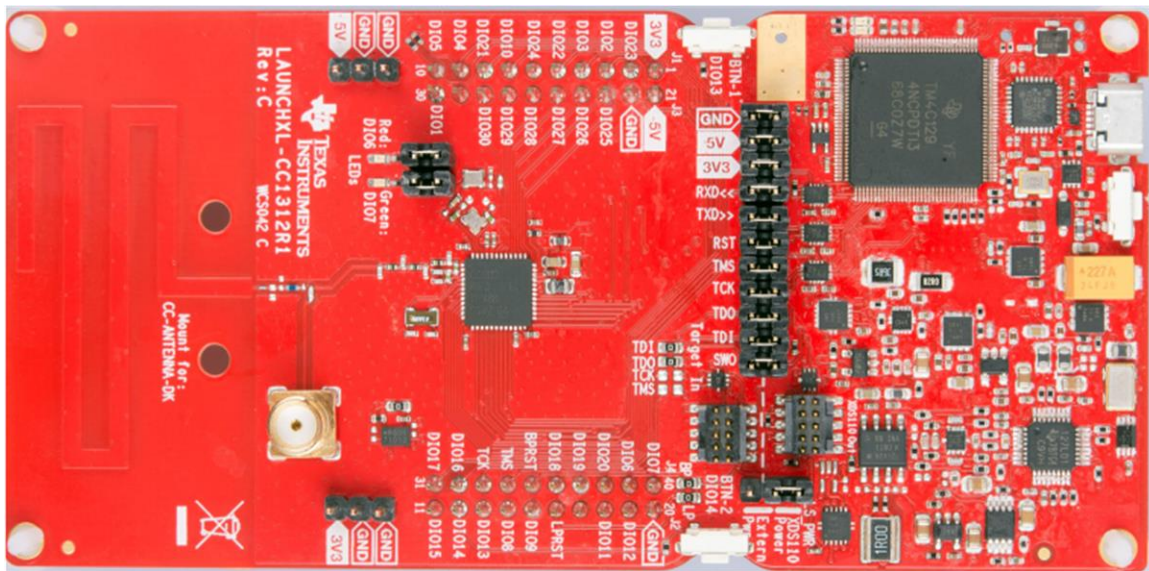
图 2. CC1312R Architecture



### 2.2.2 LAUNCHXL-CC1312R1

The [CC1312R LaunchPad™](#) is part of TI's SimpleLink MCU platform, offering a single development environment that delivers flexible hardware, software, and tool options for customers developing wired and wireless applications. The TIDA-010050 must combine with the CC1312R LaunchPad and connect with the LaunchPad kit's I/O connectors, which saves time and production cost by quickly prototyping the inductive sensing sub-system. All software examples and hardware design files included in the [SimpleLink CC13x2 SDK](#) support the CC1312R LaunchPad kit, making the development much easier.

图 3. LAUNCHXL-CC1312R1



### 2.2.3 CSD23285F5

This 29-m $\Omega$ , -12-V, P-Channel FemtoFET™ MOSFET technology is designed and optimized to minimize the footprint in many handheld and mobile applications. This technology is capable of replacing standard small signal MOSFETs while providing a significant reduction in footprint size.

## 2.3 Design Features

### 2.3.1 Ultra-Low Power Design

As smart water meters are typically battery powered, the power consumption is one of the most important specifications, where often a battery life of at least 10 years must be ensured. Besides, it should be noted that the add-on electronic modules are size constrained, so it will also limit the maximum available battery capacity. In many cases, a flow meter reports the measurement rather infrequently using the RF functionality — very often just a few times per day. Thus, it is often more challenging to keep the average current on the metrology low because the flow must be monitored continuously and will often require the MCU to wake up many times per second.

The Sensor Controller Engine (SCE) in the CC1312R device executes code from a dedicated ultra-low-leakage (ULL) RAM memory and can control peripherals independently of the main Arm® Cortex®-M4F application processor. Therefore, the main processor can sleep as long as possible and only wakes up to perform more compute-intensive tasks, like RF communication. This reduces the number of wake-ups and saves power. Updated from the CC1310, the sensor controller in the CC1312R device supports a 2-MHz clock configuration in addition to the original 24-MHz configuration. This fast wake-up and ultra-low-power 2-MHz mode is designed for energy efficient sampling, buffering, and processing both analog and digital sensor data.

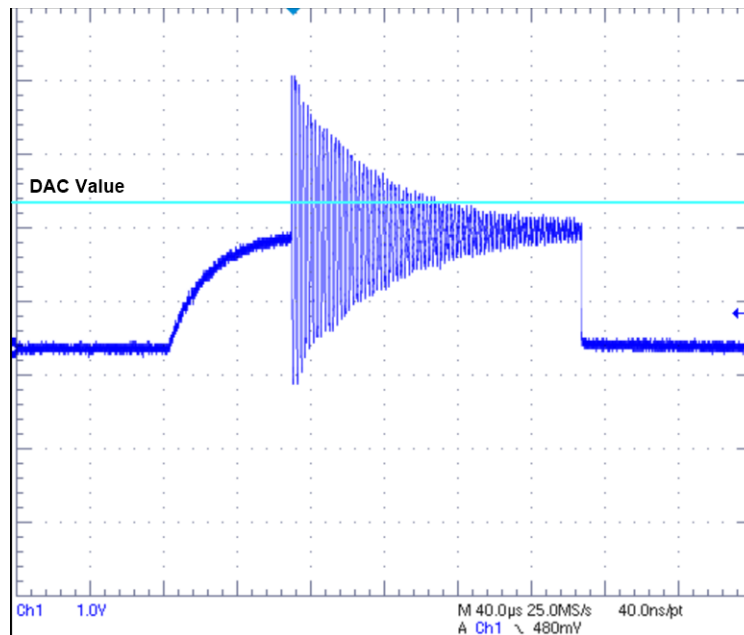
### 2.3.2 Single Chip Solution

The CC13x2 SimpleLink™ low-power RF wireless MCU products are designed toward low power in both metrology and RF communication, which means that it does not need an external RF device to implement wireless communication capability. TI offers the CC13x2 and CC26x2 wireless MCU platform with multiple wireless protocol stacks. The available stacks are both customer-modifiable and standard-based protocols, such as the Wireless M-Bus Protocol Software and the TI 15.4-Stack that is available in the [SimpleLink™ CC13x2 Software Development Kit](#).

## 2.4 LC Sensing Theory

Over time, the inductive tank (LC) sensing systems have proven their capability in industrial flow meter application. The systems are precise, cost efficient, and do not consume much power. Also, LC sensors can be calibrated to different environments, and the precision of the rotation measurement can meet Class 1 accuracy for water meters.

图 4. LC Sensor Oscillation

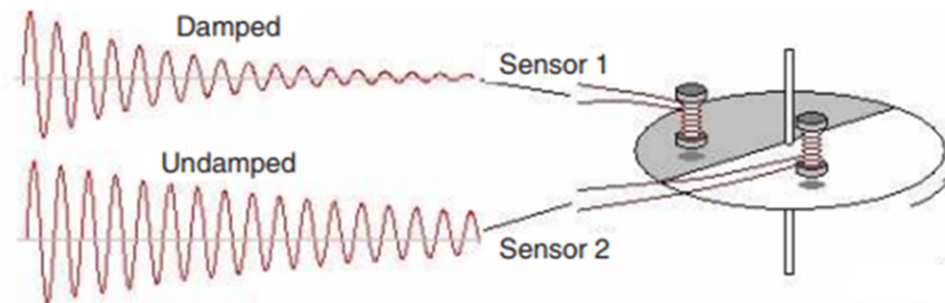


The LC oscillation theory has been introduced in the [Low-power water flow measurement with inductive sensing](#) and [Water meter for two LC sensors using Extended Scan Interface \(ESI\) reference designs](#). The LC sensor is able to detect a conductive material in the proximity of the inductor. As shown in 图 4, after triggered by an excitation pulse, the LC oscillation is generated. The oscillation signal is fed to the COMPA of the Sensor Controller Engine. Here the reference DAC is used as a programmable voltage reference for the comparator. Then, with the help of a pulse counter for the digital output signal of the comparator, the number of pulses larger than the DAC value is obtained.



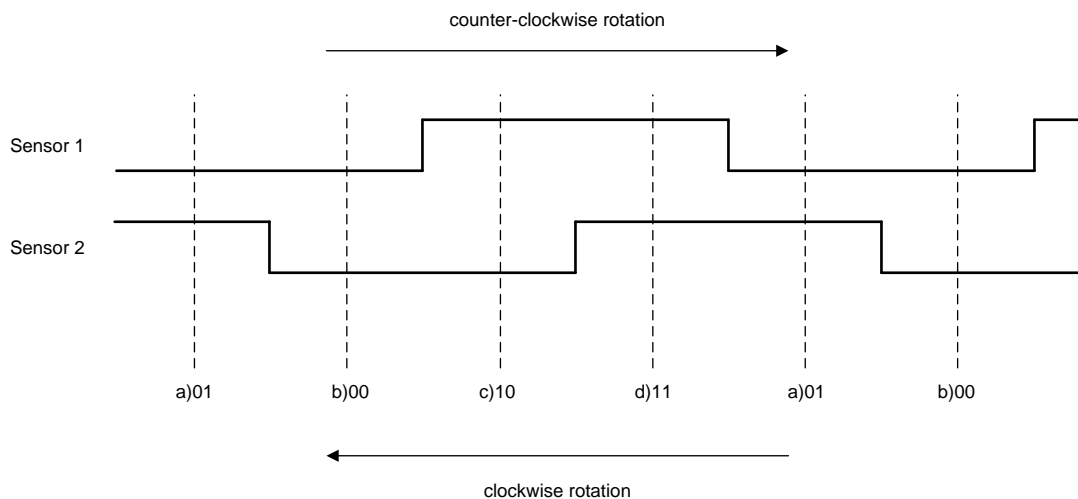
The inductor of a LC circuit is placed above the rotating disc, which is half covered with a metal coating, as shown in 图 5. The oscillating magnetic field created in the LC sensor will induce eddy currents in the metal half of the disc, which absorbs the energy from the inductor. When the inductor is above the metal part, the oscillation amplitude will decay faster, so the collected number of pulses will be substantially lower compared to the case without metal. A threshold value can be used to differentiate between damped and undamped conditions, which correspond respectively to a metal or non-metal material being in front of the LC sensor. The binary 1 is used to represent the undamped oscillation where the pulse count is more than the threshold value, while 0 is for damped condition.

图 5. Damped and Undamped Oscillation



One LC sensor can measure the rotation, but a second LC sensor is needed to detect the direction of the rotation. The flow can go in both directions in water meters due to the pressure change when an open tap is closed, so it is important to detect and calculate any flow in the reverse direction as well. The inductors are placed in a 90° off-axis angle above the disc. When the disc rotates, the measurements produce a 2-bit gray-code, where each code corresponds one quadrant of a full rotation. 图 6 shows a simple state machine with the digitized signal for a rotating disc using two LC sensors, giving out four states for one turn: 00, 01, 11, and 10. The sequence of these four states provides the direction of rotation.

图 6. State Machine During Rotation

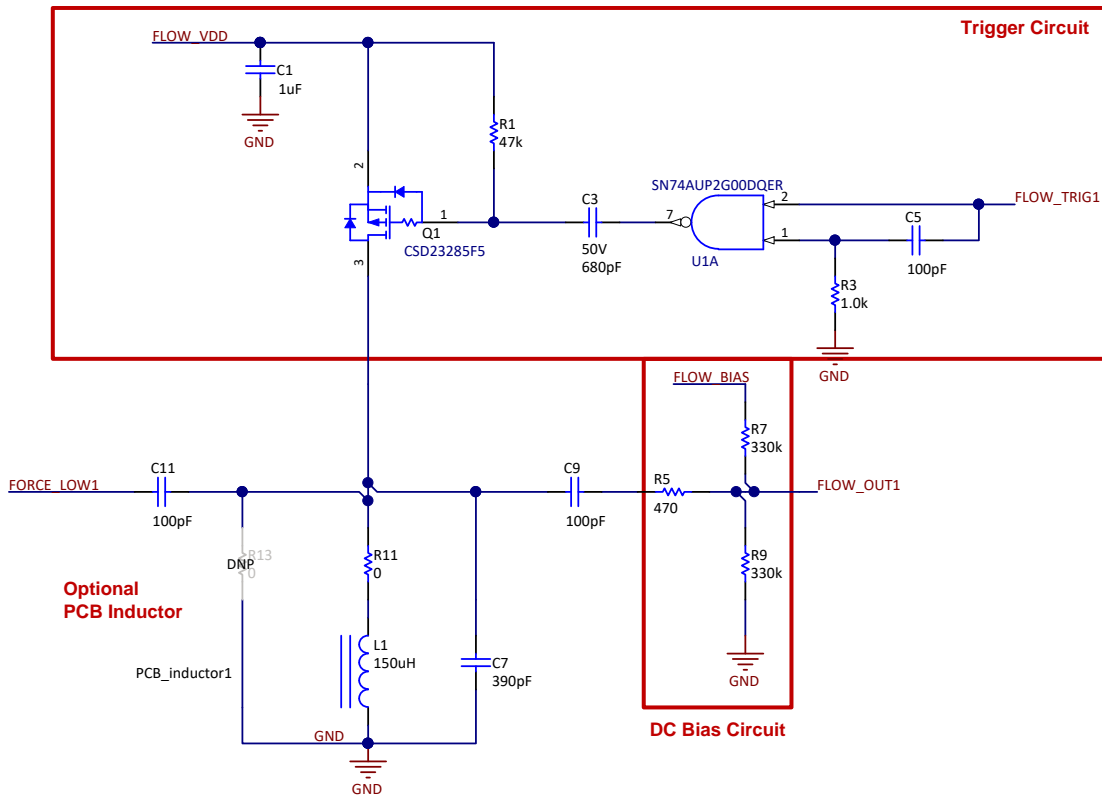


### 3 Getting Started Hardware and Software

#### 3.1 Hardware Design

In this section, key points for the TIDA-010050 board will be demonstrated. 图 7 shows the schematic of one LC sensor that can be divided into 4 parts: LC sensor, trigger circuit, DC bias circuit, and coupling effect suppression circuit. To optimize the component selection, a simulation model based on SIMatrix/SIMPLIS is provided.

图 7. Schematic of One LC Sensor



##### 3.1.1 LC Sensor Selection

Several key factors should be taken into consideration in selecting suitable component parameters for the LC tank.

- **Power consumption**

As is mentioned in the [Method to select the value of LC sensor for MSP430 Extended Scan Interface application report](#), the average power consumption for an LC sensor can be derived as

$$P_{avg} = f_s * V^2 * (C + \frac{\Delta t^2}{L}) \tag{1}$$

In 公式 1,  $f_s$  is the sampling rate and  $\Delta t$  is the duration of excitation time. The equation shows that larger L-values and smaller C-values can reduce the overall current consumption. However, the losses of the copper resistance of the inductor are neglected in the presented equations, and they have to be considered. As the inductor value increases, the copper resistance also increases. Besides, a higher resistance leads to a fast damping of LC oscillation signal. Therefore, a suitable inductor value with a smaller copper resistance is preferred.



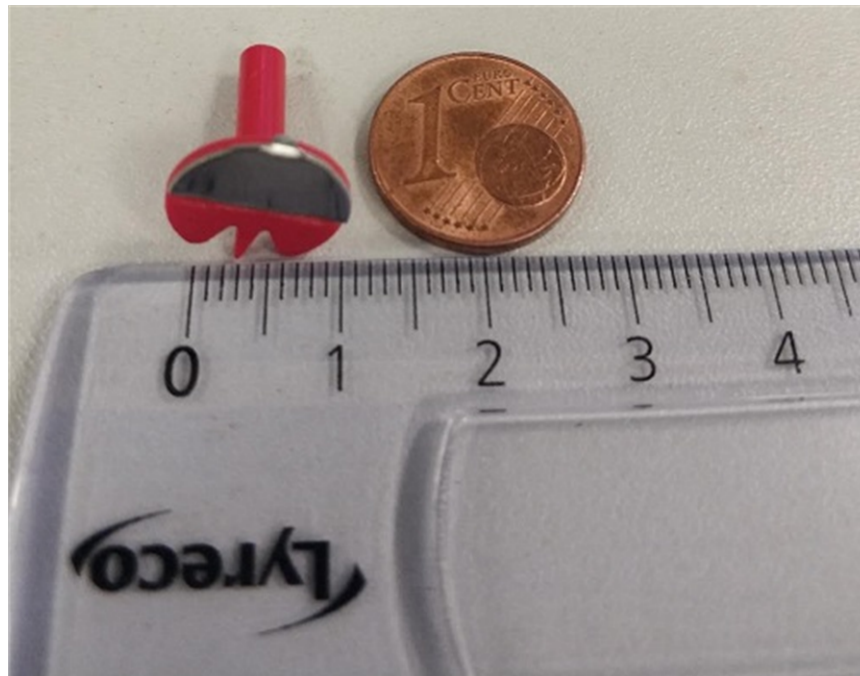
- **Oscillation frequency**

Because the COMPA performance is limited to 1 MHz, the oscillation frequency of the LC tank has to be less than that value. Alternatively, the slower the resonant frequency is, the longer the process of measuring and evaluating the oscillation will be. This also affects the energy consumption because the sensor controller engine of the CC1312R device must be powered as long as the measurement is ongoing.

- **Size and form**

The physical size of the capacitor is small. However, the inductor is much bigger. It is challenging when choosing an inductor of higher value. The inductor size is limited by the targeted rotation disc of the water meter, which is generally small. 图 8 shows a common rotation disc in actual application, which is also used in the TIDA-010050. The diameter is measured as 11 mm.

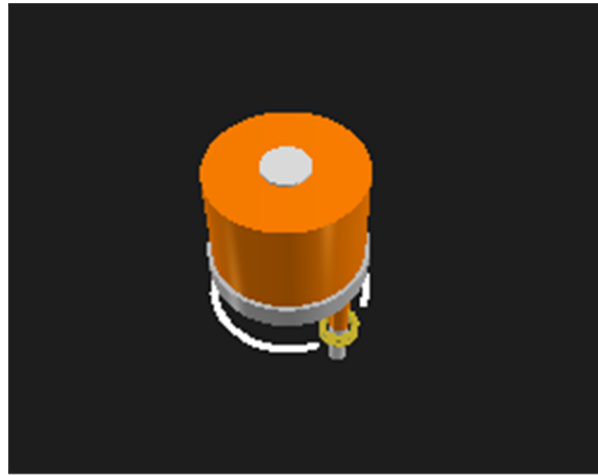
图 8. Rotation Disc



The detection performance, like distance and accuracy, is related to the area of the rotor plate covered with the magnetic field generated from the inductor. If the effective covering area is not enough, the magnetic energy absorption rate of inductor through the eddy current on the metal portion of the rotor plate is reduced. In this case, 11 mm means that the inductors used for the LC sensors can not be much wider than 5 to 6 mm in diameter.

Alternatively, the form of the inductor also plays an important role in detection performance. The dampening effect should be as large as possible to correctly differentiate between damped and undamped conditions. Thus, the electromagnetic field projected should be far and strong enough to cover the metal area of the rotation disc. In this case, shield-type inductors are not suitable in this application. In the TIDA-010050, the inductor from Gemphil, [GT1302-0](#), is implemented, and 图 9 shows its model. The inductor has a T-shaped cross-section with windings around the center.

图 9. Model of Gemphil Inductor



### 3.1.2 Trigger Circuit

As shown in 图 7, the CSD23285F5 P-Channel FemtoFET™ is used as a switch to charge the LC sensor circuitry when receiving an LC excitation pulse. The most important consideration here is to ensure that the LC circuit is enabled long enough to get fully charged. The required length of the trigger time depends on various factors such as the effective capacitance of the LC sensor and the supply voltage used. The LC excitation pulse is generated from the NAND gate, triggered by the digital IO pin of the CC1312R device and RC circuit. In the [Low-power water flow measurement with inductive sensing reference design](#), the trigger signal was directly provided from the IO pin of the CC1310, and the trigger time of 250 ns was used. For one trigger event, the trigger pin should be driven HIGH for a single processing unit and then released. Because the sensor controller in the CC1312R device uses a 2-MHz clock for low power mode, the duration for the HIGH state is 1  $\mu$ s (each CPU instruction takes 2 clock cycles). Therefore, the RC circuit here is used to provide a shorter trigger time. Different RC parameters can be implemented for different trigger time requirements.

### 3.1.3 DC Bias Circuit

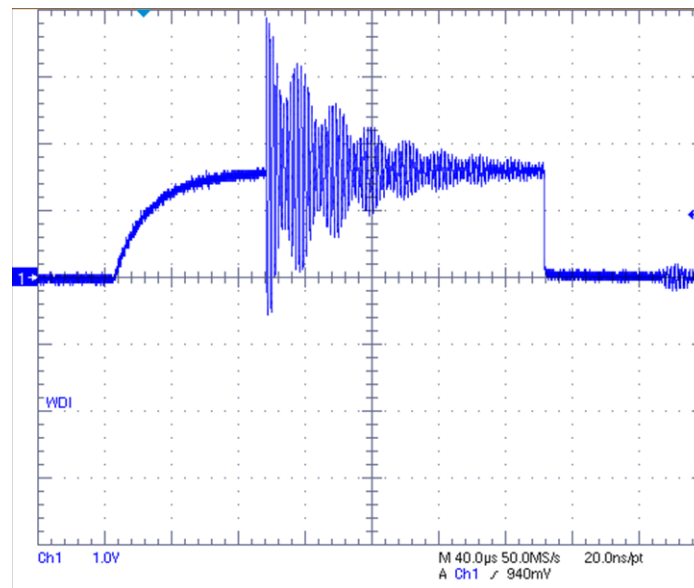
In this design, the DC bias circuit is used to level shift the common-mode level of the oscillating signal from the flow meter from GND to  $V_{DD}/2$  to limit the signal within the maximum and minimum allowed input voltage on the IO pins of the CC1312R device. The DC bias circuit also plays an important role in providing a stable and predictable signal to the on chip comparator, as shown in 图 7.

The capacitor C9 in this case is used to decouple the DC offset of the oscillation signal. The two resistors generate a specific offset. Generally, as a simple voltage divider, the resistor value can be selected as high as possible to reduce the leakage current for the power consumption concern. However, since FLOW\_BIAS voltage is only provided in such a short time during measurement for the power consumption concern, smaller leakage current will cause longer settling time to make the common-mode voltage level stable. At the same time, the leakage current will also affect the oscillation signal amplitude that bigger current will increase the damp effect. Thus, a trade off needs to achieve on both oscillation amplitude and common-mode settling time, and it is not recommended to use a resistor value less than 1 M $\Omega$  in this case.

### 3.1.4 Coupling Effect Suppression Circuit

In actual application, the rotation disc in the flow meter is generally small. Thus, to achieve a better detection performance with a fully covered sensing dimension, it is necessary to have two inductors installed in close proximity to each other. Therefore, there will be an issue in that the inductive coupling will distort the oscillation severely. 图 10 shows the oscillation result of the inductive coupling effect. Although the inductor is triggered one after another, the energy will charge back and forth from this sensor to the other one mounted next to it. The worst case is that the oscillations will be distorted too much to be able to correctly detect whether the oscillation is damped or not.

图 10. Oscillation Result of the Inductive Coupling Effect



It is possible to select different resonant frequencies for two LC sensor circuits, which can reduce the coupling effect to some extent. However, two different sensors generally will cause different detection capabilities, which may need additional tune effort to achieve optimal performance. Otherwise, the detection distance and accuracy will be limited.

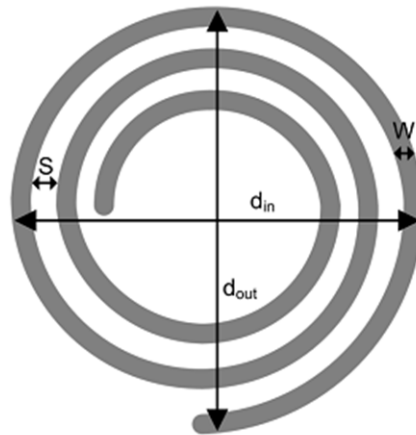
In the TIDA-010050, another solution is proposed and has been validated. Both terminals of the inductor will be forced to the same potential while the other inductor is oscillating, which can inhibit the undesired oscillation to a large extent with no current flowing. Thus, two IO pins of FORCE\_LOW and FLOW\_OUT signal will change to a low level simultaneously after the present oscillation is finished. 图 4 has shown the oscillation result with coupling effect suppression circuit enabled.

### 3.1.5 Optional PCB Inductor

As shown in 节 3.1.1, the inductor without shield from the Gemphil is implemented in the TIDA-010050. There is another possibility to provide an inductor for the LC sensor, where the inductor coils are directly fabricated onto the system PCB itself. By default, the Gemphil inductors are mounted in the board with 0-Ω resistors R11 and R12 installed. If using the PCB inductor for the evaluation, R13 and R14 must be mounted instead.

图 11 shows an example of the geometry of a PCB coil, where  $d_{in}$  represents the inner diameter of the coil,  $d_{out}$  represents the outer diameter of the coil,  $W$  represents the trace width of the coil, and  $S$  represents the spacing between the traces used in the coils.

图 11. PCB Coil Geometry



In the TIDA-010050, the [Coil Designer tool](#), a WEBENCH tool originally used for the LDC0851 solution, is used to facilitate PCB coil design. This tool was developed initially to create a reference and sense coil design, which can be exported to CAD files, as an initial version for this design. 图 12 shows one example of setting the page for the coil design. Because the size of the coil is limited by the detection area,  $d_{out}$  is set to 7.5 mm. The final inductance value depends on factors such as diameter of the coil, the number of turns of the coil, the number of coil layers, as well as the distance between the coil layers. To increase the inductance, more turns and layers with smaller trace width ( $W$ ) is preferred. However,  $W$  should be adjusted to consider the minimum trace width supported by the PCB manufacturer for the design. 4 mils is chosen in this design.

图 12. Coil Design Setting Page

### Select Coil Geometry And Other Parameters

Metric Imperial Oz-Cu: ON OFF

LC sensor capacitance(C)  pF  
min: 10 - max: 10000

Outer diameter of inductor(D<sub>out</sub>)  mils  
min: 42 - max: 5900

Turns per layer(N)  Turns  
min: 1 - max: 120

Trace width(W)  mils  
min: 2 - max: 40

Spacing between traces(S)  mils  
min: 2 - max: 12

Copper thickness(t)  oz-Cu  
min: 0.5 - max: 5

Temperature(T)  °C  
min: -40 - max: 125

Space between 1<sup>st</sup> layer and 2<sup>nd</sup> layer(x12)  mils  
min: 1 - max: 60

Space between 2<sup>nd</sup> layer and 3<sup>rd</sup> layer(x23)  mils  
min: 1 - max: 60

Space between 3<sup>rd</sup> layer and 4<sup>th</sup> layer(x34)  mils  
min: 1 - max: 60

Output Parameters		
Name		Output
Total inductance - Circular	<i>i</i>	3.16 μH
Sensor frequency	<i>i</i>	15091.15 kHz
Q factor	<i>i</i>	50.65
AC resistance (skin effect only)	<i>i</i>	4.18 Ω
Coil fill ratio	<i>i</i>	0.24
Coil inner diameter (D <sub>in</sub> )	<i>i</i>	71.28 mils
DC resistance	<i>i</i>	0.99 Ω
Average diameter	<i>i</i>	183.28 mils
Geometric mean diameter	<i>i</i>	0.61
Self inductance per layer	<i>i</i>	0.84 μH
Coil length per layer	<i>i</i>	8061.08 mils
Skin depth	<i>i</i>	0.66 mils
Self resonant frequency	<i>i</i>	56.67 MHz
Resonance impedance	<i>i</i>	11109.67 Ω
Current	<i>i</i>	0.13 mA
Power dissipation	<i>i</i>	0.23 mW

4 layers are implemented for the PCB inductor. However, the inductors outputted from the Coil Designer tool are 2 independent inductors with 2 layers, respectively. Thus, further modification is needed to combine the inductors into one, and the physical construction of a 4-layer inductor has been demonstrated in the TIDA-00828, as shown in 图 13. To increase the mutual coupling between inductors, the circular coil should use the same current flowing direction through it in every layer. 图 14 shows the connection process of coils on 4 different layers. Coils on the signal 2 layer and bottom layer should be exchanged first, due to the current flowing direction requirement.

On the TIDA-010050 board, there are 3 PCB inductors, where the third one generally works as a back up inductor in case one of them is damaged. In this design, the value of the PCB inductor is measured as 15 μH, with a high resistor value of 4.7 Ω. With a fast decay speed for the oscillation, the measurement can not be well supported. Thus, further design effort and evaluation is recommended to optimize the solution with PCB inductor.

图 13. 4-Layer Inductor Physical Construction

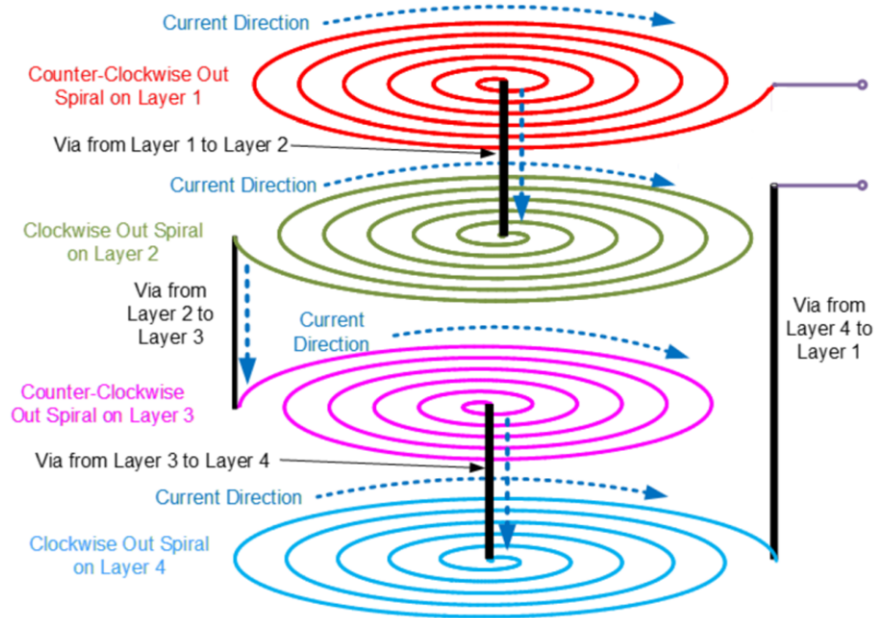
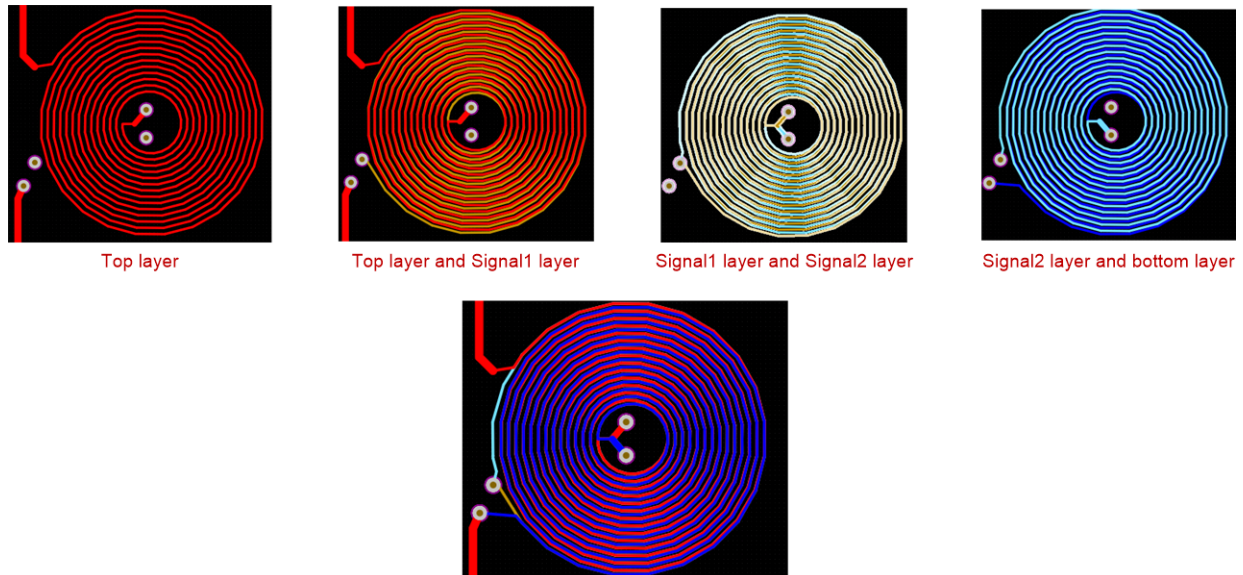


图 14. Connection Process of Coils on 4 Different Layers



### 3.1.6 Simulation Model

A simulation model is provided based on SIMetrix/SIMPLIS, which is an easy-to-use professional tool for analog circuit design. The model is fast, accurate, and has reliable convergence. With the multi-step analysis function, it is very convenient to tune different parameters to achieve better system performance.



图 15. Simulation Model for One LC Sensor

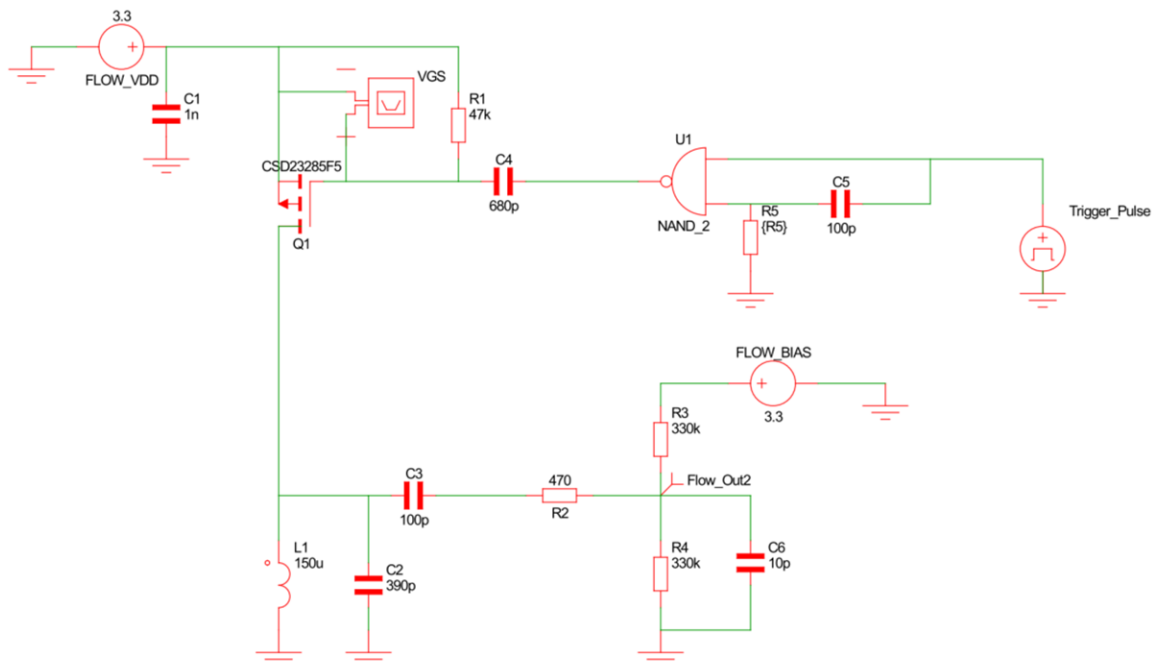


图 15 shows the simulation model for one LC sensor. In the simulation model, the Trigger\_Pulse is used for the trigger signal with an excitation time of 1  $\mu$ s. A capacitor of 10 pF is added towards GND on the Flow\_Out2 to simulate the capacitance induced by routing and the input capacitance within the CC1312R device, like ESD diodes. Because there is no simulation model for the MCU chip, the decoupled capacitors are not presented in the simulation model due to the model integrity check.

A simulation example is given for the influence of different parameters of R5 in the trigger circuit. Here, a multi-step analysis function will be used. The steps are shown in 图 16. Firstly, double click on R5 and enter the value R5. Then click *Simulator, Enable multi-step, Setup Multi-step, Define List*, and OK. Finally, the simulation result with different parameter steps of R5 can be obtained, as shown in 图 17. The effective trigger time is measured by the time of  $V_{GS} > V_{GS(th)}$  (typically  $-0.65$  V) of the CSD23285F5. With cursors toggle On/Off tool, the trigger time can be measured as 51 ns, 139 ns, and 227 ns for  $R5 = 1$  k $\Omega$ , 3 k $\Omega$ , and 5k $\Omega$ , respectively.

图 16. Simulation Steps of Multi-step Analysis Function

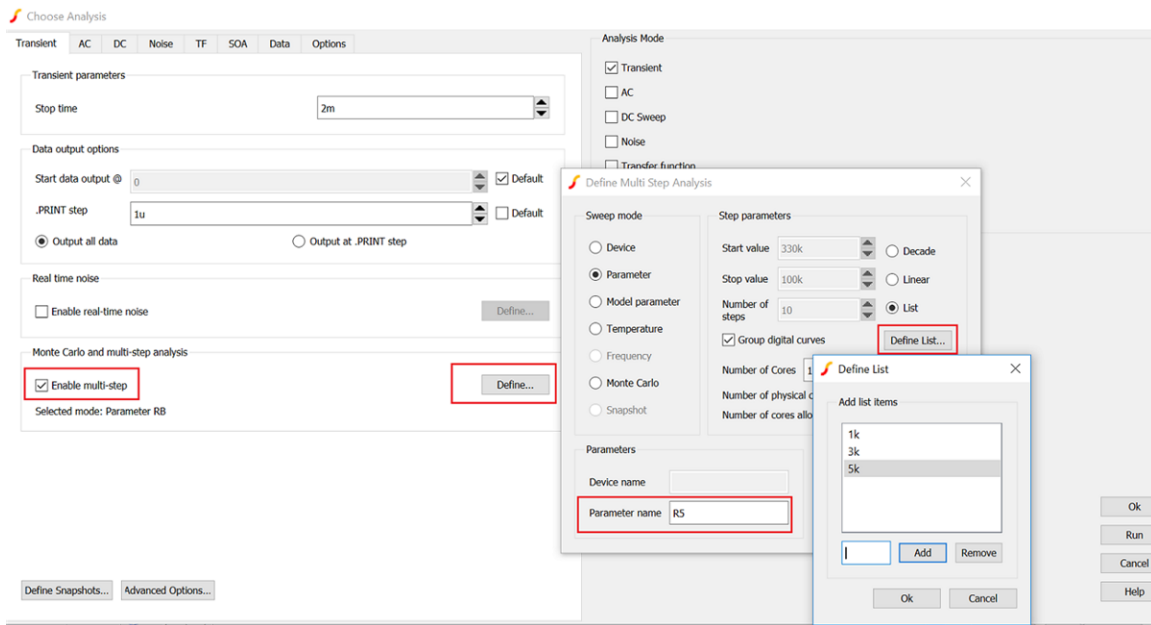
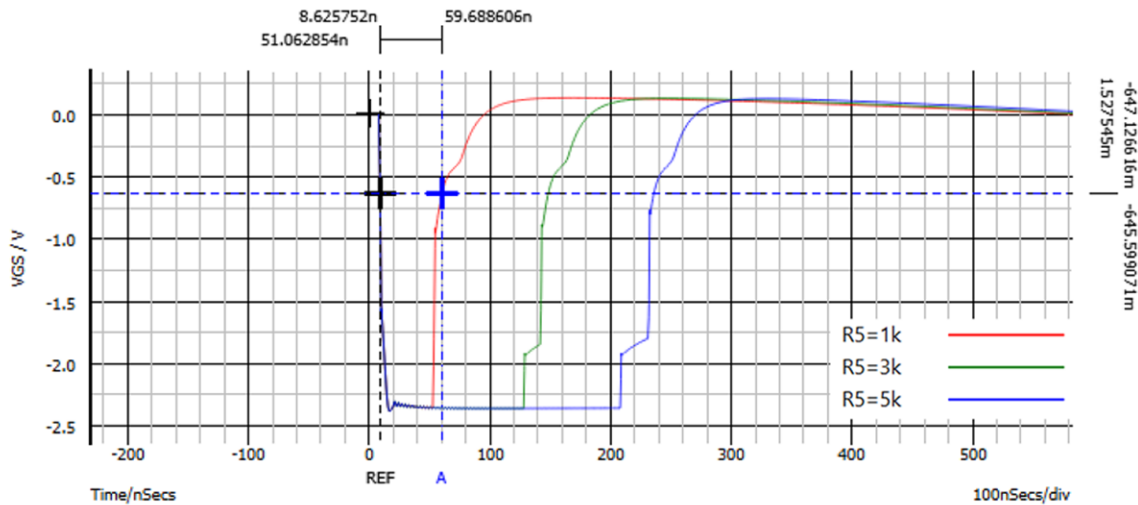


图 17. Simulation Result With Different Parameter Steps of R5



## 3.2 Software

The released software projects for the TIDA-010050 include two parts. The first is a Sensor Controller Studio (SCS) code for controlling the two LC sensors. The second is a complete CCS source code, which builds upon TI-RTOS and incorporates the SCS code portion. The development tools of SCS version 2.4.0 or later and Code Composer Studio (CCS) version 8.2.0 or later are available for free on product pages. Because the design is developed based on the SimpleLink platform, it is necessary to download and install [SIMPLELINK-CC13X2-26X2-SDK](#) as the source files for the previously mentioned software projects.

Both firmware code projects for SCS and CCS are provided as a single-source code deliverable on the [TIDA-010050 tool folder](#). The CCS source code project contains the SCE project, found in the install path `/TIDA-010050_SW/sce/` and named `LC_sensor.scp` which handles the LC sensing part. Ensure that the sensor controller output project in SCS is saved to the CCS project folder in the Code Generator Panel. How to integrate a sensor controller project into an application can be found in the CC13x2 SimpleLink Academy training or [SCS Getting Started Guide](#).

In SCS, it is possible to run the LC sensing project with run-time logging (debug mode), which provides a generic, easy-to-use environment for evaluating and optimizing performance of tasks while these run at full speed. After that, CCS code is needed to integrate the task into a fully standalone application and flashed into the chip.

In the TIDA-010050 CCS firmware, the system CPU will wake up for the alert from the sensor controller task. Whenever the rotation count or error count changes, the CPU will be alerted to indicate the related information by blinking LEDs.

图 18. Flowchart for LC Sensing Control in SCE

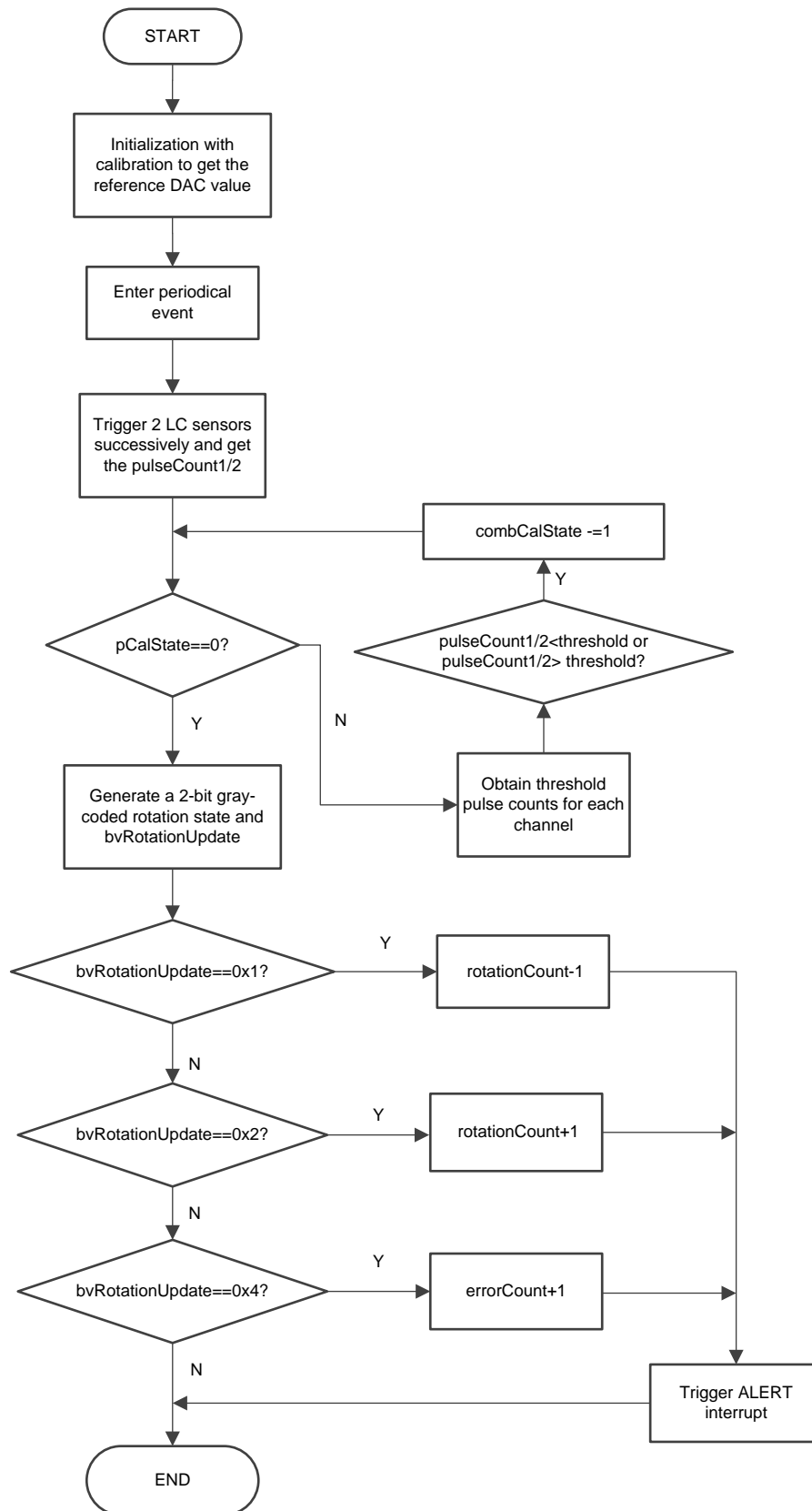


图 18 shows the flowchart for LC sensing task in SCE. In the Constants and Data Structures Panel in SCS, there are user-defined parameters which can be tuned for the performance evaluation and optimization, as listed in 表 2.

**表 2. Parameters for LC Sensing Task**

PARAMETER	DESCRIPTION
REFDAC_OFFSET	Offset added to reference DAC calibration result during initialization.
CAL_MIN_MAX_DIFF	Least required difference between minimum and maximum pulse count. Higher value represents stronger robust for the detection accuracy.
execlInterval	Belong to cfg data structure, to decide the sampling rate.

The LC sensing task consists of two task code blocks: Initialization Code and Event Handler Code. The Initialization Code runs one time when the task is started, and the Event Handler Code is triggered after a specified delay. Further demonstration for the detailed code functions is given in the following sections.

### 3.2.1 DAC Calibration

During initialization, the reference DAC value is obtained before the LC tank oscillation is triggered. As shown in the following code, after the DC bias circuit is powered up, a DAC value that corresponds to the bias voltage is decided. Then, the reference DAC value is equal to the value derived from COMPA plus a user-defined REFDAC\_OFFSET value. A suitable REFDAC\_OFFSET value should be carefully selected to differentiate pulse count between damp and undamped conditions. With a smaller REFDAC\_OFFSET value, more pulse count can be obtained, while an unstable pulse count might be seen if REFDAC\_OFFSET is too small.

```
// Power up external circuitry and peripheral modules
gpioSetOutput(AUXIO_XS_FLOW_POWER);
refdacEnable(REFDAC_PWRMODE_ANY, REFDAC_REF_VDDS);
compaEnable(COMPA_PWRMODE_ANY);
refdacStartOutputOnCompaRef(1);

// Find the Reference DAC output value for each channel
U16 auxioFlowOutput = AUXIO_AXD_FLOW_OUTPUT_1;
for (U16 n = 0; n < CHANNEL_COUNT; n++) {
    // Release the COMPA input node
    gpioSetOutput(auxioFlowOutput);
    compaSelectGpioInput(auxioFlowOutput);
    fwDelayUs(1000);
    // Until the COMPA output goes high ...
    U16 refdacOutput = 0;
    do {
        // Increase reference DAC output by 1
        refdacOutput += 1;
        refdacChangeOutputValue(refdacOutput);
        fwDelayUs(100);

        // Check the COMPA output
        U16 compaValue;
        compaGetOutput(compaValue);
    } while (compaValue != 0);

    // Save the result
    state.pRefdacOutput[n] = refdacOutput + REFDAC_OFFSET;
    // Clamp the COMPA input node
    gpioClearOutput(auxioFlowOutput);

    auxioFlowOutput = AUXIO_AXD_FLOW_OUTPUT_2;
}
```

```

}
// Power down external circuitry and peripheral modules
gpioClearOutput(AUXIO_XS_FLOW_POWER);

```

### 3.2.2 Pulse Count Threshold Calibration

After initialization, the rotation detection starts to run, and the threshold pulse counts should be decided to differentiate the damped and undamped conditions. Thus, during the two first rotations, the minimum and maximum pulse counts are updated and the threshold is set to the middle value. As mentioned previously, CAL\_MIN\_MAX\_DIFF is used to make sure the enough difference for the pulse count obtained during damped and undamped conditions. In the test, CAL\_MIN\_MAX\_DIFF=3 is selected to achieve the maximum detection distance with acceptable accuracy. Initially, output.pCalState is set to 4 for the calibration iteration to also confirm that the selected threshold value is the correct one. The rotation count will not update until the calibration process is completed.

```

// For each channel ...
for (U16 n = 0; n < CHANNEL_COUNT; n++) {
    if (output.pCalState[n] != CAL_STATE_DONE) {
        U16 meas = output.pMeasPulseCount[n];
        U16 min = state.pMinPulseCount[n];
        U16 max = state.pMaxPulseCount[n];
        if (meas < min) {
            min = meas;
            state.pMinPulseCount[n] = meas;
        }
        if (meas > max) {
            max = meas;
            state.pMaxPulseCount[n] = meas;
        }
        // If the difference between minimum and maximum is sufficient ...
        output.diff[n] = max - min;
        // U16 diff = max - min;
        // if (diff >= CAL_MIN_MAX_DIFF) {
        if (output.diff[n] >= CAL_MIN_MAX_DIFF) {
            // Require the measured value to be above and below thresholds around the
            // mid-point two times. Each time, decrement calState
            if (output.pCalState[n] & 0x01) {
                U16 thres = ((max + min) >> 1) - (CAL_MIN_MAX_DIFF >> 1);
                if (meas < thres) {
                    output.pCalState[n] -= 1;
                }
            } else {
                U16 thres = ((max + min) >> 1) + (CAL_MIN_MAX_DIFF >> 1);
                if (meas > thres) {
                    output.pCalState[n] -= 1;
                }
            }
        }
    }
}

```



### 3.2.3 Trigger and Sampling

The following code shows the trigger and sampling mechanism for the first LC tank. After powering up the DC bias circuit and peripheral modules, the oscillation is triggered by releasing the trigger IO pin for a single processing unit and driving the pin low for a single processing unit. A delay is expected to wait for the DC bias voltage to be stable, shown as `fwDelayUs(10)`. After oscillation occurs, the pulse counter is used to count the number of oscillations on the COMPA input, which is larger than the reference DAC value. Thus, with the expected pulse count, 2-bit gray-coded rotation state named `rotationState` can be updated by comparison with the threshold value. Finally, both `Flow_Output` and `Force_Low` pins will be driven low, to suppress the inductive coupling effect and wait until the next trigger is enabled.

```
// Power up external circuitry and peripheral modules
gpioSetOutput(AUXIO_XS_FLOW_POWER);
compaEnable(COMPACT_PWRMODE_ANY);
refdacEnable(REFDAC_PWRMODE_ANY, REFDAC_REF_VDDS);

// CHANNEL 1
// Release the flow output node and connect it to COMPACT
gpioSetOutput(AUXIO_AXD_FORCE_LOW_1);
gpioSetOutput(AUXIO_AXD_FLOW_OUTPUT_1);
compaSelectGpioInput(AUXIO_AXD_FLOW_OUTPUT_1);

// Start the COMPACT reference, and wait for it to stabilize
refdacStartOutputOnCompactRef(state.pRefdacOutput[CHANNEL_1]);
refdacWaitForStableOutput();
fwDelayUs(10);

// Enable the pulse counter and generate the trigger
pcntEnable(PCNT_INPUT_COMPACT);
gpioSetOutput(AUXIO_O_FLOW_TRIGGER_1);
gpioClearOutput(AUXIO_O_FLOW_TRIGGER_1);

// Count pulses until no new pulses have occurred for 10 us
fwDelayUs(10);
pulseCount = 0;
do {
    fwDelayUs(10);
    prevPulseCount = pulseCount;
    pcntGetValue(pulseCount);
} while (pulseCount != prevPulseCount);

// Save the result and convert to rotation state
output.pMeasPulseCount[CHANNEL_1] = pulseCount;
output.threshold[CHANNEL_1] = (state.pMinPulseCount[CHANNEL_1]+state.pMaxPulseCount[CHANNEL_1])>>
1;
if (pulseCount > output.threshold[CHANNEL_1]) {
    rotationState |= 0x1;
}

// Clamp the Flow_Output and Force_Low node
gpioClearOutput(AUXIO_AXD_FLOW_OUTPUT_1);
gpioClearOutput(AUXIO_AXD_FORCE_LOW_1);
```

### 3.2.4 Rotation State Decoding

During initialization, a look-up table of rotation state machine is defined by one 16-bit word for each rotation state.

```
state.pRotationFsm[0] = 0x4010; // Decrement: 00->01, Error: 00->11
state.pRotationFsm[1] = 0x0402; // Increment: 01->00, Error: 01->10
state.pRotationFsm[2] = 0x0040; // Error: 10->01
state.pRotationFsm[3] = 0x0004; // Error: 11->00
```

During the rotation detection operation, the rotation counter is updated based on the new rotation state and last rotation state. In the code, `bvRotationUpdate` is derived for the new rotation state based on the previous rotation state. The rotation counter has 3 effective values: 0x1, 0x2, and 0x4, representing decrement, increment, and all possible errors, respectively. 表 3 shows the relationship between rotation state and `bvRotationUpdate`. Therefore, it can be concluded that increment and decrement is only decided by 01->00 and 00->01, respectively, during one rotation turn. The following code shows that the task in the sensor controller core will wake up the CPU every time the event of increment, decrement, or if an error occurs. How to interface with the CPU can be modified according to different custom applications.

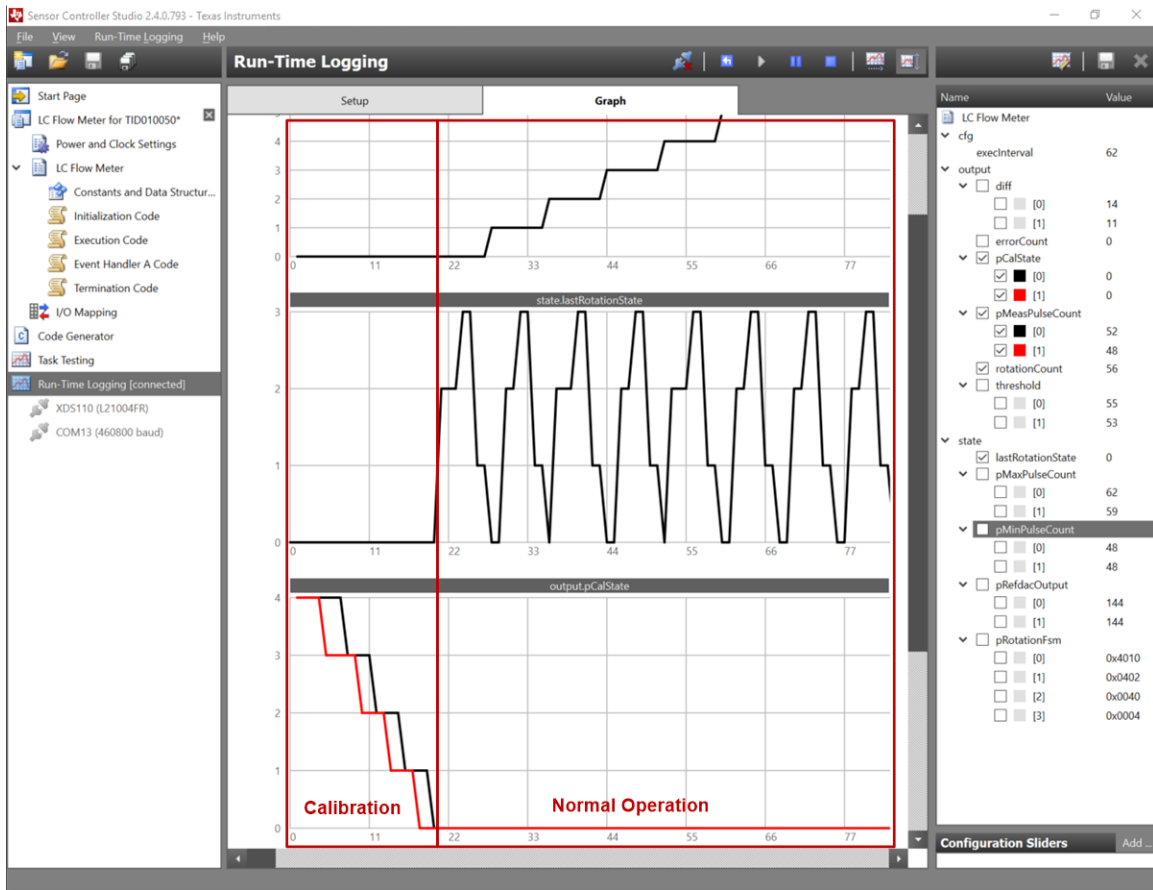
```
// Update the rotation and error counters
U16 n = state.lastRotationState;
state.lastRotationState = rotationState;
U16 bvRotationUpdate = (state.pRotationFsm[n] >> (rotationState << 2)) & 0xF;
if (bvRotationUpdate == 0x1) {
    output.rotationCount -= 1;
    fwGenAlertInterrupt();
} else if (bvRotationUpdate == 0x2) {
    output.rotationCount += 1;
    fwGenAlertInterrupt();
} else if (bvRotationUpdate == 0x4) {
    output.errorCount += 1;
    fwGenAlertInterrupt();
}
```

**表 3. Relationship Between Rotation State and `bvRotationUpdate`**

LAST ROTATION STATE	NEW ROTATION STATE	<code>bvRotationUpdate</code>	MEASUREMENT RESULT
00	01	0x1	Decrement
	10	0x0	-
	11	0x4	Error
01	00	0x2	Increment
	10	0x4	Error
	11	0x0	-
10	00	0x0	-
	01	0x4	Error
	11	0x0	-
11	00	0x4	Error
	01	0x0	-
	10	0x0	-

图 19 shows a complete view of a run-time logging session with both calibration and normal operation. The sampling rate is 100 Hz by default, and it can be changed by `cfg.execlInterval` mentioned in 表 2. The sampling rate is decided by the specified delay in AUX Timer 1 to trigger execution of the Event Handler code. Because the timer runs off of 4-kHz ticks generated by the RTC, the sampling rate of 100 Hz is derived with the `cfg.execlInterval` equal to 40.

图 19. Run-Time Logging With Both Calibration and Normal Operation



## 4 Testing and Results

### 4.1 Test Setup

#### 4.1.1 Rotation Measurements Setup

图 20. Test Platform Setup

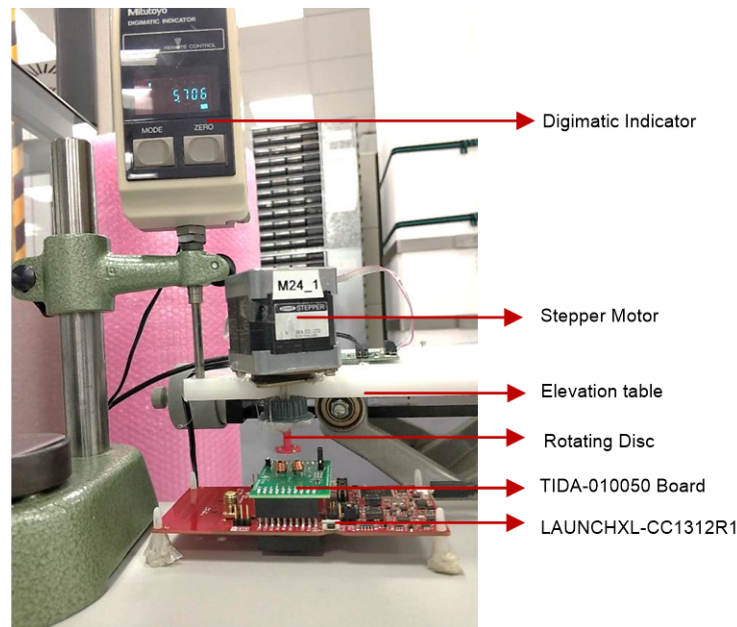


图 20 shows the test platform for the TIDA-010050. An *off-the-shelf* stepper motor based on the [DRV8846EVM](#) is used to simulate various speeds for the rotating disc, which is glued to the motor shaft. The motor can be configured with 200 steps per full turn with a fully controlled rotation speed. The motor is fixed to the white elevation table. The TIDA-010050 board is connected together with the CC1312R LaunchPad kept in a fixed position, where two inductors are positioned exactly below the rotating disc.

The setup was carefully created as it has to achieve a reproducible distance between the disc and the LC sensors, which can be precisely measured. This is achieved by the combination of an elevation table, whose height above the workbench can be continuously adjusted with a turning knob. A digimatic indicator of the Mitutoyo device is set to 0 mm when the disc touches the inductors and indicates the distance between the disc and inductors when the table is elevated to the desired testing distance. The resolution of the digimatic indicator is 1  $\mu\text{m}$ , which is more than sufficient as this distance in mechanical meters will often have a tolerance of 0.1 mm or greater.

The XY-placement of the two inductors against the rotating disc will have a great influence on the measurement performance. Some fine-tuning is needed to find the best position for the disc and inductors. In a real application, this issue is mitigated because the electronic add-on module can be easily designed to fit exactly above the disc.

## 4.1.2 Board Configuration

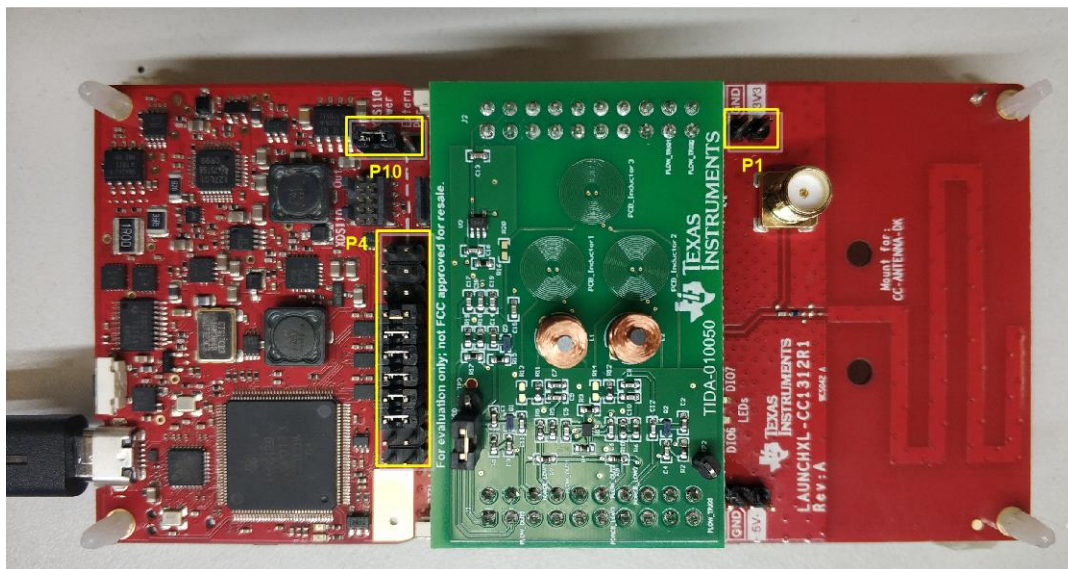
The recommended evaluation step is to run the example first in the run-time logging panel in SCS and check that it works as expected with the rotating disc. The rotation measurement accuracy can be evaluated. After that, the board can be tested without an on-board XDS debugger using a USB connector, with external power supply instead, to obtain the power consumption data accurately. Thus, there are three different board configuration options during the test.

### 4.1.2.1 Test With Run-Time Logging Powered by USB

The LaunchPad LAUNCHXL-CC1312R1 is designed to be powered from a USB-compliant power source by default. A LDO powered from the USB VBUS supply supplies 3.3 V to the XDS debugger, the CC1312R device and associated circuitry. If using this test mode, before starting any run-time logging sessions, it is important to confirm the following hardware setup for jumpers on the LaunchPad, as shown in 图 21:

- 3V3, RXD, TXD, RESET, TMS, and TCK are mounted. Remove the other jumpers in the main jumper block P4.
- A jumper is mounted in the position marked XDS110 power in P10.

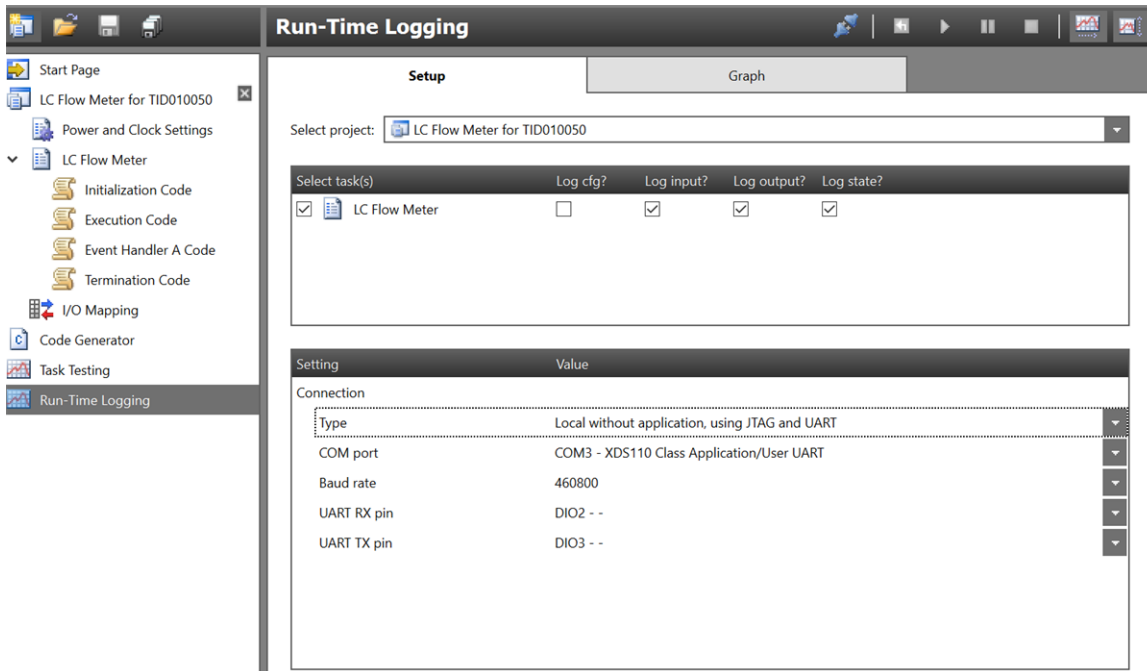
图 21. Hardware Setup for Jumpers on the LaunchPad



Use the following steps in SCS, as shown in 图 22.

- Navigate to the run-time logging page.
- Select the sensor controller project in the installed path/ TIDA\_010050\_SW/sce/LC\_sensor.scp.
- Configure the connection settings: verify that the COM port corresponds to your device's application and user UART port.
- Click the connect button when all setting have been properly configured.
- Start run-time logging by clicking the start button.

图 22. Run-Time Logging Setting



#### 4.1.2.2 Test With Run-Time Logging Powered by External Supply

In this mode, it is possible to validate the performance with different voltage supplies, since the detection accuracy can be observed with run-time logging. Ensure that the voltage applied stays within the supply range of the CC1312R device (1.8~3.8 V). The following hardware setup for jumpers on the LaunchPad is required:

- RXD, TXD, RESET, TMS and TCK are mounted. Remove the other jumpers, especially 3.3 V, in the main jumper block P4.
- Move the jumper to the position marked Extern. Pwr in P10, and connect the external supply to the 3V3 pin on P1.

#### 4.1.2.3 Test With Standalone Mode Powered by External Supply

After the CC1312R device is successfully flashed with CCS project combined with SCE project, an external supply can be provided at the 3V3 pin on P1, without the USB connector. It is necessary to test with this mode to obtain the power consumption data accurately.

Before downloading the code into the chip, make sure the latest SCE project has been saved to the CCS project folder. It can be confirmed with clicking *View output directory* in the Code Generator panel in SCS.

For the hardware setup, all the corresponding jumpers on the main jumper block P4 near to XDS110 debugger must be removed, and the P10 jumper should be in the XDS110 power position or removed.



## 4.2 Test Results

### 4.2.1 Power Consumption Measurements

In many cases, a flow meter reports the measurement rather infrequently using the RF functionality — often just a few times per day. However, it is often more challenging to achieve the low average current on the measurement. In this section, the power consumption for the TIDA-010050 has been investigated with the hardware setting shown in 节 4.1.2.3.

Because the CC1312R device is running with low power mode, periodic recharge of the VDDR will bring current spikes, which are challenging to capture with common multimeter equipment. The N6705B DC power analyzer is used to measure the current precisely. To measure the power purely with the metrology process, the CPU will not be waken up because the disc is not rotating during measurement, while the disc should position with the metal part faced to only one inductor. The obtained value can represent the result of average scenario for 4 rotation states during normal operation. In this test, the Gemphil inductor GT1302-0 of 150  $\mu\text{H}$  with LC tank capacitor of 390 pF are used.

图 23. Result Captured by N6705B DC Power Analyzer

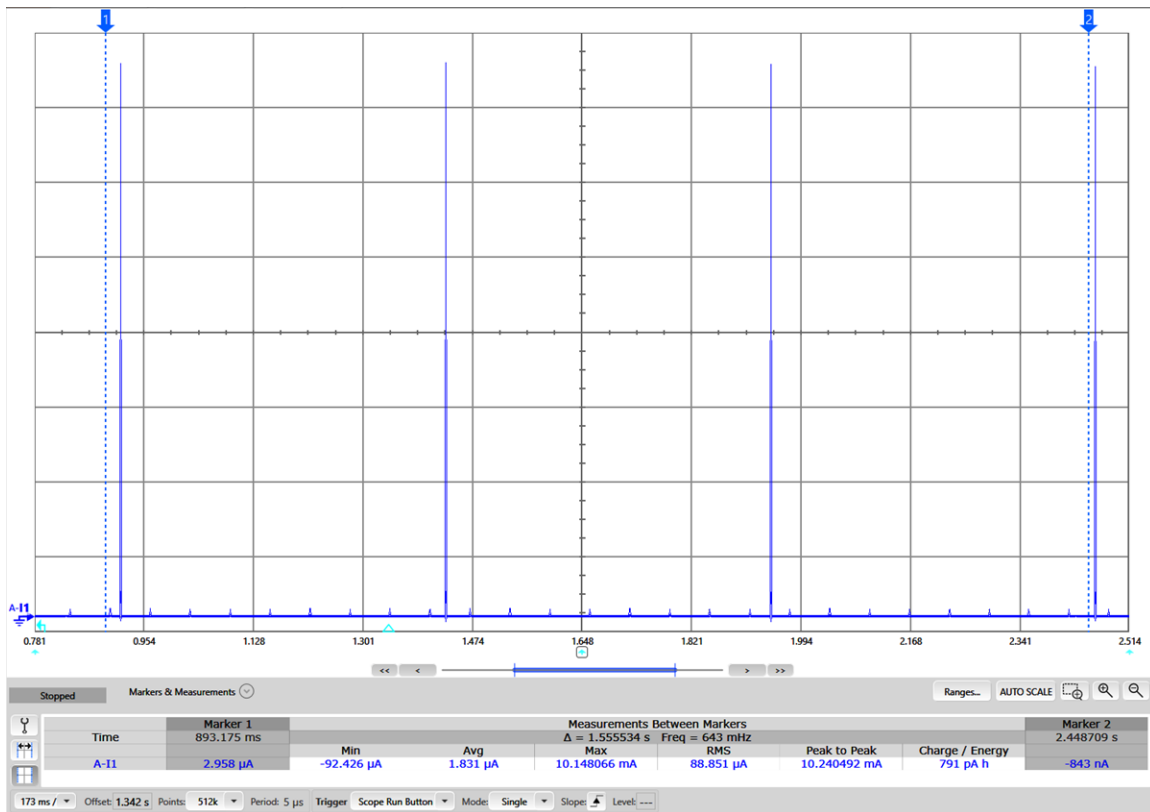
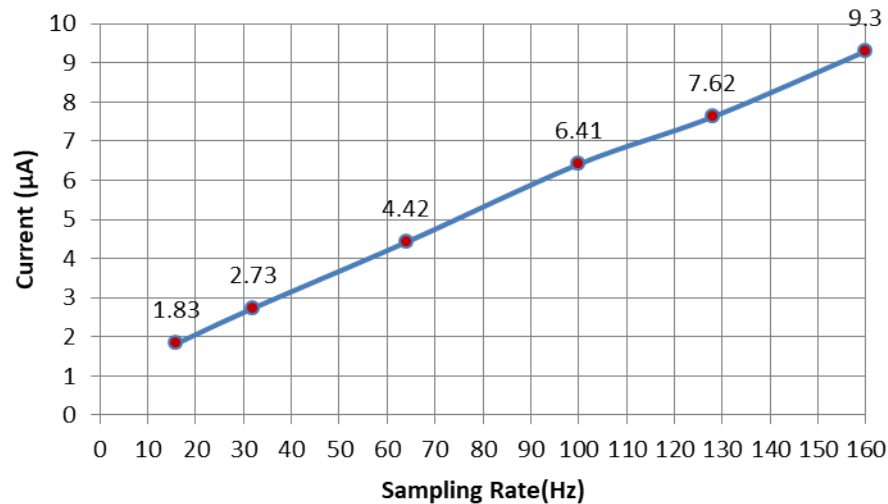


图 23 shows the result captured by the N6705B DC power analyzer with a 16-Hz sampling rate, where 3 recharge pulses are included within 1.55 s measurement time, and the average current of 1.83  $\mu\text{A}$  is obtained. Further test results of different sampling rates are given with 3.3-V power supply, shown in 图 24. Different sampling rates are needed for different maximum flow rates depending on the mechanical construction and the pipe diameter of the water meter. It is also common to use two different sampling rates in the water meter for zero flow condition and maximum flow rate, generally with 16 Hz and 64 Hz or greater, respectively. Compared to the power consumption results in the TIDA-01228 with the CC1310 device, it has been validated that the TIDA-010050 with the CC1312R device can save power to a larger extent.

图 24. Power Consumption With Different Sampling Rates



Because smart meters are commonly powered by a battery, like Li-SOCL2 or LiMnO2, the battery voltage will change with discharging throughout its lifetime. Generally, LiMnO2 cells start with up to 3.2-V open circuit voltage and have a typical cut-off voltage at 2 V, whereas LiSoCl2 start at approximately 3.8 V open circuit voltage and get discharged down to 3.2 or 3.1 V over the lifetime.

Therefore, further tests with the supply voltage ranging from 2 to 3.8 V have been conducted. 表 4 shows the results with different voltages using sampling rate of 64 Hz. Thus, it can be concluded that the current value is almost constant in the range of 2 to 3.8 V, so lower power consumption can be achieved at lower supply voltage, which helps extend the battery lifetime.

表 4. Power Consumption With Different Voltages

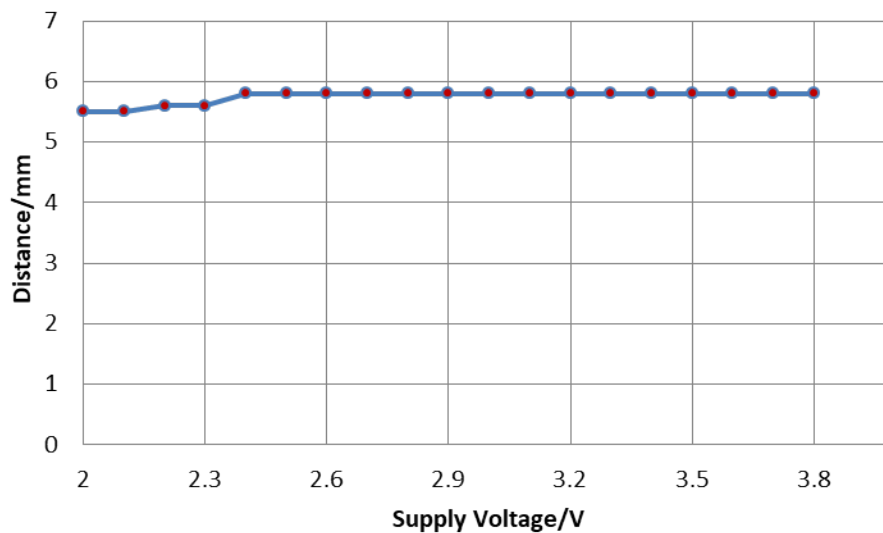
Voltage (V)	2	2.1	2.2	2.5	3	3.3	3.5	3.8
Current ( $\mu\text{A}$ )	4.52	4.63	4.76	4.27	4.43	4.42	4.53	4.8
Power ( $\mu\text{W}$ )	9.04	9.72	10.47	10.67	13.29	14.59	15.86	18.24

#### 4.2.2 Distance Between Inductors and Rotating Disc

Because the rotating disc is normally behind a glass or plastic cover, the LC sensor inductors will always be a few millimeters away. It is much more convenient with larger distances for the installation with different types of mechanical meters. Thus, maximizing this distance is in general one of the most important design goals and the most difficult design challenges to overcome.

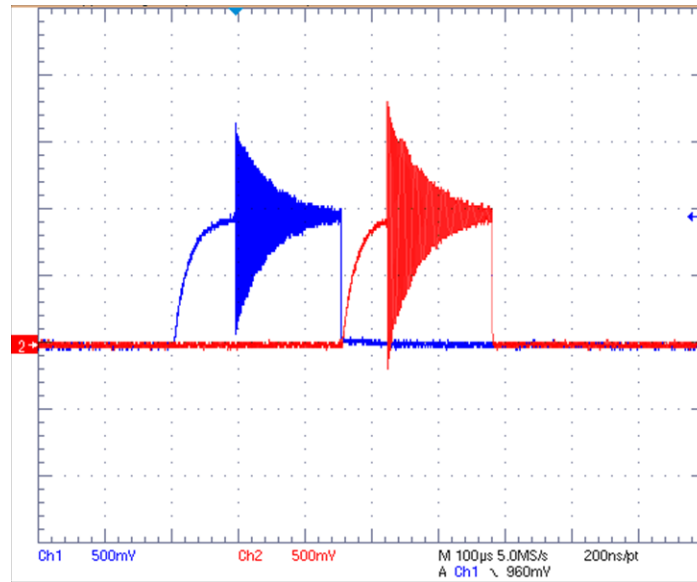
In this design, the maximum distance of 5.8 mm has been achieved between disc and inductors using the Gemphil inductor GT1302-0 of 150  $\mu$ H and the LC tank capacitor of 390 pF. Considering the voltage changing with battery discharging throughout its lifetime, it is necessary to measure the detection distance under different voltage supplies, ranging from 2~3.8 V. 图 25 shows the results of maximum distance under different voltages. In this test, the disc is configured with a rotation speed of 4 Hz, where the sampling rate is 32 Hz. As shown in 图 25, the maximum distance of 5.8 mm covers the wide range from 2.4 to 3.8 V. There will be a slight decrement for the maximum distance when the supply voltage goes down to 2.3 V or lower, with 5.5 mm at 2 V.

**图 25. Results of Detection Distance Under Different Voltages With the Gemphil Inductor**



According to the oscillation result shown in 图 26, with a supply voltage of 2 V, the oscillation amplitude for the first LC tank has decreased compared to the second one. The reason is that when the voltage drops down, it takes more time to power up the DC bias circuit, so more delay is needed before triggering the first channel to wait until the bias voltage becomes stable. Except for this decrease, the maximum detection distance performance is stable along with the full voltage range of both Li-SOCL2 and LiMnO2 battery. Therefore, the solution has an excellent detection distance margin because the distance requirement of 3~5 mm is common for water meters.

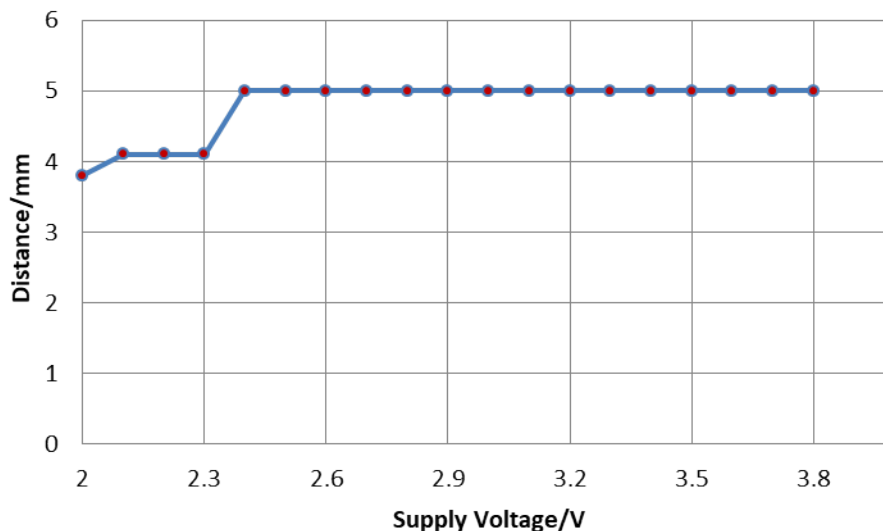
图 26. Oscillation Result With 2-V Voltage Supply



With the voltage going down, the optimal threshold pulse count might slightly change, so TI suggests running the calibration when the voltage changes. The battery monitor function in the CC1312R makes it possible to detect the battery voltage during operation and to trigger the recalibration if needed.

As mentioned in 节 3.1.1, different types of inductors will have different detection performance. In this test, another Murata inductor of 470  $\mu\text{H}$  is also tested, with an LC tank capacitor of 220 pF, using the same sampling rate of 32 Hz. 图 27 shows the results of maximum detection distance under different voltages with the Murata inductor. In this case, the maximum distance of 5 mm has been achieved, while the performance during lower voltages decreases to a larger extent, with 3.8 mm at 2 V. It can be improved with increasing the delay time (fwDelayUs) before triggering the first LC tank mentioned in 节 3.2.3, but it may cause higher power consumption due to longer power up time of the DC bias circuit.

图 27. Results of Detection Distance Under Different Voltages With Murata Inductor



### 4.2.3 Rotation Measurement Accuracy

Using the DRV8846EVM and a standard stepper motor with 200 steps per full rotation, it is possible to test different turning speeds from 1 turn to 10 turns per second (1 Hz~10 Hz) to simulate the disc rotation of flow meters. To detect the rotation number under different rotational frequencies, the LC sensor should adjust the sampling rate accordingly. Meanwhile, as mentioned previously, an increasing sampling rate will cause higher power consumption, so a minimum sampling rate should be derived.

According to EN ISO 4064-1:2014-11 – 1/3, a water meter shall be designed with the ratio of highest and lowest flow rate, which is selected in the defined list, generally 40, 80, 100, and so forth. Thus, with the flow rate varies in different water usage conditions, the measurement accuracy should meet the requirement at highest flow rate with the required minimum sampling rate.

Use the following equation for the minimum sampling rate calculation of a system with two sensors and a 180° covered plate:

$$\text{Sampling Rate}_{min} = 2 \times \frac{360}{\theta} \times \text{Rotation Frequency} \quad (2)$$

In 公式 2,  $\theta$  represents the angle between the two sensors (in this case, 90°). The parameter 2 represents oversample to guarantee the accuracy.

In the test, using run-time logging mode with SCS, different sampling rates can be configured and rotation measurement results can be observed. As the DRV8846 GUI control settings support only 16-bit values, the maximum steps possible are 65k. For the tests, 60k steps were used resulting in 300 full turns with different speed settings. The rotation measurement results are shown in 表 5, where the supply voltage is 3.3 V with 5.8-mm detection distance, using the Gemphil inductor GT1302-0, LC tank capacitor of 390 pF. For each test with different disc rotation speeds, the disc is controlled to start and stop after 300 turns at the same position, where the inductors are faced to non-metal part of the disc, with rotation state of 11, and the tested disc rotation speeds cover many types of mechanical water meters. The results indicate that this solution can achieve Class 1 measurement accuracy requirements (error<1%) of ISO4064-1:2014-11, using the minimum sampling rates for different rotation speeds.

**表 5. Rotation Measurement Results (Targeted 300 turns)**

ROTATION SPEED (Hz)	SAMPLING RATE (Hz)	MEASUREMENT RESULT (turns)	ERROR
4	32	300	0
6	48	300	0
8	64	300	0
10	80	300	0

It is important to ensure the distance between the two inductors and their mechanical position is stable. In the TIDA-010050 design, this is achieved through the soldering of the Gemphil inductors to the PCB. If stranded wire inductors are used, such as the Gemphil inductor GT1301-0, then these inductors must be somehow mechanically fixed either through plastic enclosure or some other means, which keep them firmly fixed above the rotating disc.

#### 4.2.4 RF Functionality Demonstration

The LC-sensor metrology is implemented completely in the ultra-low-power Sensor Controller Engine of the CC1312R Wireless MCU, leaving both the RF-core and Cortex®-M4F core fully available for host applications and RF communications. Although the RF connectivity solution itself is not part of this reference design, the CC1312R device can be used for adding RF protocol support in the Sub-1 GHz or 2.4-GHz band or even both bands if either the CC1352R or CC1352P dual-band RF device is used. Multiple RF protocol stacks like wM-Bus, 6LoWPAN or BLE can be integrated to achieve a single-chip AMR module for mechanical flow meters. See the [SimpleLink MCU Platform](#) for more details.

## 5 Design Files

### 5.1 Schematics

To download the schematics, see the design files at [TIDA-010050](#).

### 5.2 Bill of Materials

To download the bill of materials (BOM), see the design files at [TIDA-010050](#).

### 5.3 PCB Layout Recommendations

There are no strict layout requirements to be considered. To use for custom applications, both hardware designs of [TIDA-010050](#) and [LAUNCHXL-CC1312R1](#) should be for reference. If using normal inductors for the solution, the hardware part of PCB inductor can be ignored.

#### 5.3.1 Layout Prints

To download the layer plots, see the design files at [TIDA-010050](#).

### 5.4 Altium Project

To download the Altium Designer® project files, see the design files at [TIDA-010050](#).

### 5.5 Gerber Files

To download the Gerber files, see the design files at [TIDA-010050](#).

### 5.6 Assembly Drawings

To download the assembly drawings, see the design files at [TIDA-010050](#).

### 5.7 Simulation Model

To download the assembly drawings, see the design files at [TIDA-010050](#).

## 6 Software Files

To download the software files, see the design files at [TIDA-010050](#).

## 7 Related Documentation

1. Texas Instruments, [Low-power water flow measurement with inductive sensing reference design](#)
2. Texas Instruments, [Method to select the value of LC sensor for MSP430 extended scan interface \(ESI\) application report](#)
3. Texas Instruments, [SimpleLink™ CC1312R LaunchPad™ for 868 MHz/915 MHz bands LAUNCHXL-CC1312R1 application report](#)
4. Texas Instruments, [CC26xx, CC13xx sensor controller studio version 2.4 .0 getting started guide](#)
5. Gemphil Technologies, Inc., Inductor [GT1302-0](#), [GT1301-0](#)

### 7.1 商标

E2E, SimpleLink, LaunchPad, FemtoFET are trademarks of Texas Instruments.  
Altium Designer is a registered trademark of Altium LLC or its affiliated companies.  
Arm, Cortex are registered trademarks of Arm Limited.  
Wi-SUN is a registered trademark of Wi-SUN Alliance, Inc.  
ZigBee is a registered trademark of ZigBee Alliance.



All other trademarks are the property of their respective owners.

## 7.2 Third-Party Products Disclaimer

TI'S PUBLICATION OF INFORMATION REGARDING THIRD-PARTY PRODUCTS OR SERVICES DOES NOT CONSTITUTE AN ENDORSEMENT REGARDING THE SUITABILITY OF SUCH PRODUCTS OR SERVICES OR A WARRANTY, REPRESENTATION OR ENDORSEMENT OF SUCH PRODUCTS OR SERVICES, EITHER ALONE OR IN COMBINATION WITH ANY TI PRODUCT OR SERVICE.

## 8 Terminology

**Water meter** — Mechanical water meters with impeller and a rotating disc in their dial, which can be sensed to measure its rotation speed and direction (thus the water flow)

**Inductive or LC sensing** — Using an LC tank oscillation to detect a nearby metal plate (mounted on the rotating disc) through dampened oscillations due to induced eddy currents

**Rotating disc** — Small circular disc, with a half-round metal plate, often used as 1 liter dialindicator, found in many mechanical flow meters in the world

**Class 1 or Class 2** — Precision categories for water meters defined in DIN EN ISO 4064-1:2014-11. In Europe, water meters are designed according to the EN ISO 4064 specifications, which are closely related to OIML R-49 documents, used in other regions of the world as well. The measurement error defines if the Meter is either Class 1 with  $\pm 1\%$  maximum error or Class 2 with  $\pm 2\%$  error from 0.1°C to 30°C. For the temperatures above 30°C, the maximum permissible error is increased to  $\pm 2\%$  or  $\pm 3\%$  for Class 1 or 2 respectively.

## 9 About the Author

**AKI LI** is a Field Application Engineer in China, who got his master degree of Electrical Engineering in Zhejiang University. During the rotation program in TI's Grid Infrastructure team, he worked with Milen for the development of this reference design.

**MILEN STEFANOV** (M.Sc.E.E) is a system engineer at TI, working in the Grid Infrastructure field and an expert in RF communication technologies and metering applications. After graduating, he spent 5 years as a research assistant at the University of Chemnitz (TUC) and 3.5 years in the semiconductor industry in high-speed optical and wired communications as a system engineer. He joined TI in 2003 to become a Wi-Fi © expert and support TI's Wi-Fi products at major OEMs. Since 2010, he has focused on metering and Sub-1 GHz RF solutions for the European Grid Infrastructure market. Mr. Stefanov has published multiple articles on wM-Bus technology in Europe and presented technical papers at the Wireless Congress and Smart Home & Metering summits in Munich.

## 重要声明和免责声明

TI“按原样”提供技术和可靠性数据（包括数据表）、设计资源（包括参考设计）、应用或其他设计建议、网络工具、安全信息和其他资源，不保证没有瑕疵且不做任何明示或暗示的担保，包括但不限于对适销性、某特定用途方面的适用性或不侵犯任何第三方知识产权的暗示担保。

这些资源可供使用 TI 产品进行设计的熟练开发人员使用。您将自行承担以下全部责任：(1) 针对您的应用选择合适的 TI 产品，(2) 设计、验证并测试您的应用，(3) 确保您的应用满足相应标准以及任何其他功能安全、信息安全、监管或其他要求。

这些资源如有变更，恕不另行通知。TI 授权您仅可将这些资源用于研发本资源所述的 TI 产品的应用。严禁对这些资源进行其他复制或展示。您无权使用任何其他 TI 知识产权或任何第三方知识产权。您应全额赔偿因在这些资源的使用中对 TI 及其代表造成的任何索赔、损害、成本、损失和债务，TI 对此概不负责。

TI 提供的产品受 [TI 的销售条款](#) 或 [ti.com](#) 上其他适用条款/TI 产品随附的其他适用条款的约束。TI 提供这些资源并不会扩展或以其他方式更改 TI 针对 TI 产品发布的适用的担保或担保免责声明。

TI 反对并拒绝您可能提出的任何其他或不同的条款。

邮寄地址：Texas Instruments, Post Office Box 655303, Dallas, Texas 75265

Copyright © 2022，德州仪器 (TI) 公司